Abdominal Radiology

Published online: 02 July 2018

Abdom Radiol (2019) 44:936–949
https://doi.org/10.1007/s00261-018-1686-x

MRI evaluation of pancreatic ductal adenocarcinoma: diagnosis, mimics, and staging

Andrew W. Bowman [1] and Candice W. Bolan[1]

[1]Department of Radiology, Mayo Clinic, 4500 San Pablo Road, Jacksonville, FL 32224, USA

Abstract

The radiologist's role in the evaluation of pancreatic ductal adenocarcinoma remains critical in the management of this deadly disease. Imaging plays a vital role in the diagnosis and staging of pancreatic cancer. Although CT is more commonly used for staging pancreatic cancer, MR is increasingly playing an important role in this regard. In our institution, all pancreatic malignancies undergo staging with MRI. In this pictoral essay, we illustrate the MR imaging features of pancreatic ductal adenocarcinoma and its mimics, and we also discuss pearls and pitfalls in MR staging of pancreatic carcinoma.

Key words: Pancreas cancer—Adenocarcinoma—MRI

Pancreatic ductal adenocarcinoma is a common malignancy, with the American Cancer Society estimating over 55,000 new cases and over 44,000 deaths in the United States in 2018 [1]. Despite advances in treatment, the mean 5-year survival remains 8%. However, the stage of pancreatic adenocarcinoma is an important prognostic indicator, as the 5-year survival for localized disease is 32% [2]. This highlights the importance of accurate staging of pancreatic adenocarcinoma.

From the radiologist's perspective, diagnosing and staging pancreatic cancer can be challenging. In the axial plane, the pancreas is frequently in the very center of the patient's abdomen, ensconced in the duodenal sweep and deep to both the stomach and colon. Vital vascular structures for solid and hollow viscera flank the pancreas. Additionally, by the nature of the disease, pancreatic adenocarcinoma frequently is poorly marginated and poorly enhancing. This hampers detection of involvement of adjacent organs and vascular structures, which confers drastic changes in treatment and prognosis. Not surprisingly, it has been reported that over 50% of surgeries performed for curative resection encounter locally advanced or metastatic disease not detected on pre-operative imaging [3].

Staging of pancreatic adenocarcinoma most routinely is performed with multiphase contrast-enhanced computed tomography (CT), given its ready availability, high spatial resolution, and reproducibility [4]. For local staging of pancreas cancer, magnetic resonance imaging (MRI) performs comparably to CT [5]. Given its superior soft-tissue characterization, however, MR may be better suited for small masses or isoattenuating masses not well appreciated on CT [6, 7]. MR has also demonstrated increased sensitivity for detection of metastatic disease, particularly that involving the liver [8]. Consequently, MR has become the modality of choice at our institution for staging pancreas cancer [9]. The purpose of this pictorial essay is to share our approach and experience using MRI to diagnose pancreatic adenocarcinoma, to illustrate pancreas cancer mimics, and to stage disease.

Technique

All of our pancreas cancer exams are performed on a 3T MR scanner (Siemens Skyra, Berlin, Germany) using a torso coil. All patients fast for at least 4 h before the exam. The protocol and typical parameters are listed in Table 1. All patients receive a weight-based dose of gadobutrol (Gadavist, Bayer, Leverkusen, Germany) IV contrast. Importantly, 0.5 mg IV glucagon is administered immediately before contrast administration to suspend bowel peristalsis. Of note, immediately following contrast administration, two consecutive axial T1

CME activity This article has been selected as the CME activity for the current month. Please visit https://ce.mayo.edu/node/78562 and follow the instructions to complete this CME activity.

Correspondence to: Andrew W. Bowman; *email:* bowman.andrew@mayo.edu

Table 1. MR imaging parameters for pancreas cancer

Sequence	Flip angle (degrees)	Repetition time (ms)	Echo time (ms)	Slice thickness (mm)	Slice gap (mm)	Field of view
Coronal T2 SSFSE	145	1400	92	5	6	319 × 319
Axial T2 SSFSEfs	146	1400	99	5	6	210 × 320
Sagittal T2 SSFSE	130	1400	106	5	6	218 × 280
Axial in/out of phase	9	4.53	2.51/1.28	3	N/A	240 × 320
Axial DWI	90	6300	59	6	7.2	280 × 399
3D MRCP	120	1700	499	1.7	N/A	280 × 280
Thin axial T2 SSFSE	150	1200	113	4	4.4	217 × 290
Thin coronal T2 SSFSE	120	1600	118	4	4.4	300 × 300
Axial T1fs pre/post	9	3.36	1.34	3	N/A	210 × 320
Thin axial T1fs post	17	3.6	1.29	1.5	N/A	225 × 300
Coronal T1fs pre/post	9	3.31	1.25	3	N/A	318 × 340
Sagittal T1fs pre/post	9	3.38	1.28	2.5	N/A	224 × 299

SSFSE single-shot fast-spin echo, *MRCP* magnetic resonance cholangiopancreatography, *DWI* diffusion weighted imaging, *fs* with fat suppression

weighted post-contrast sequences are obtained with decreased slice thickness and a higher flip angle. The first covers the pancreas and the inferior aspect of the liver; the second covers the remaining superior aspect of the liver [9]. This technique was initially adopted to better delineate the peripancreatic vascular anatomy, and more specifically to discover variants of the hepatic arterial anatomy. However, we have also found these thinner sliced sequences with higher contrast to be extremely valuable in tumor staging, as discussed below.

Diagnosis

The majority of pancreatic adenocarcinomas arise in the pancreatic head, with approximately 25% arising in the body and tail [10]. The classic appearance of pancreatic adenocarcinoma on MRI is an irregular, T1 hypointense, poorly enhancing mass that obstructs nearby ducts, either the pancreatic duct or the common bile duct (Fig. 1). Adenocarcinomas generally demonstrate variable T2 intensity and can exhibit restricted diffusion. Adenocarcinomas that arise from malignant transformation of intraductal papillary mucinous neoplasms (IPMN) typically are cystic, T2 hyperintense lesions (Fig. 2), similar to those developing in nodular, solid components of mucinous cystic neoplasms (Fig. 3) [11–14]. Occasionally, adenocarcinomas exhibit only very subtle signal abnormalities or enhancement, with or without very mild ductal irregularities (Fig. 4) [6]. Here in particular, MRI, with superior contrast resolution and multiple sequences of varying techniques, truly can make a diagnostic impact surpassing that of CT.

Mimics

The differential diagnosis for pancreatic adenocarcinoma includes an eclectic array of pathologies [15].

Non-neoplastic mimics

Focal acute pancreatitis can appear as an irregular T1 hypointense area of poor enhancement and increased T2 signal, similar to an adenocarcinoma on initial imaging (Fig. 5) [10]. Focal pancreatitis may also demonstrate ductal obstruction, peripancreatic fat infiltration, and involvement of adjacent vascular structures [16]. Clinical presentation and laboratory evaluation can be crucial to differentiate the two pathologies. Short interval follow-up imaging exam and/or additional evaluation with endoscopic ultrasound (EUS) may also be necessary.

Groove pancreatitis, a specific type of focal chronic pancreatitis, can pose a diagnostic dilemma. Traditionally, groove pancreatitis has been divided two types, the pure form and the segmental form [17]. Both forms involve the space between the pancreatic head and the duodenum (the pancreaticoduodenal groove), though the segmental form typically extends into the pancreatic head. Its imaging appearance can range from mild inflammation about the groove to sheetlike, crescentic soft-tissue deposits in the groove, often in conjunction with medial duodenal wall thickening and/or cystic deposits within that wall [18]. Cases of significant soft-tissue deposition may be indistinguishable from pancreatic adenocarcinoma prospectively; however, suggestive imaging features include the typical location in the pancreaticoduodenal groove, medial duodenal wall thickening, and T2 hyperintense cysts in the duodenal wall or along the margin between the pancreas and the duodenum (Fig. 6). Regardless, surgical resection may be required to provide a definitive diagnosis.

Autoimmune pancreatitis (AIP) is another form of chronic pancreatitis, classically representing the pancreatic manifestation of IgG4-related disease [19]. AIP can demonstrate both focal and diffuse forms, and the focal form generally presents as a masslike lesion that is hypoenhancing relative to the rest of the pancreas on early post-contrast sequences [20]. Differentiation between focal AIP and adenocarcinoma may be impossible based on the imaging appearance of the pancreas alone. Features suggesting its diagnosis include evidence of IgG4 disease elsewhere in the body (often the biliary system), elevated serum IgG4 levels, and improvement of imaging findings following treatment with steroids.

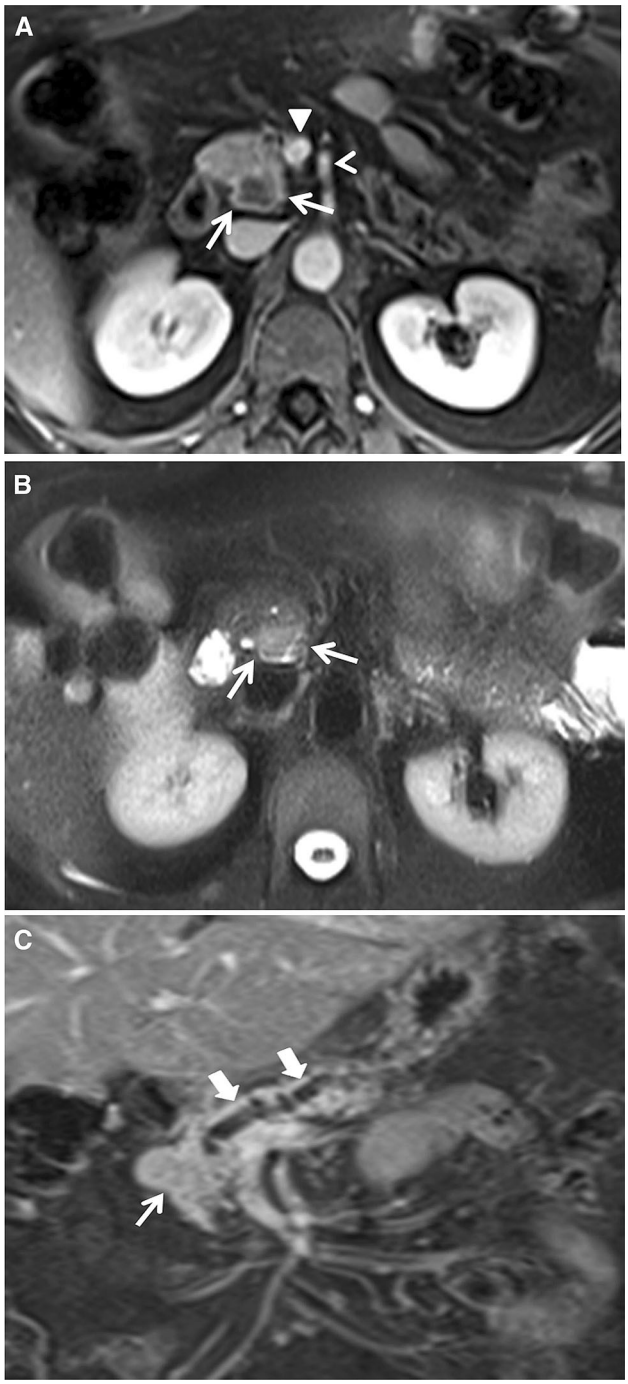

◀**Fig. 1.** Axial T1 weighted post-contrast image (**A**) demonstrating a small hypoenhancing mass in the head of the pancreas (white arrows). As was confirmed at surgery, this is a resectable tumor with no abnormal soft-tissue involvement of the nearby superior mesenteric vein (SMV, solid arrowhead) or superior mesenteric artery (SMA, open arrowhead). Axial T2 weighted fat-saturated image (**B**) at the same level illustrates increased T2 signal within the mass (arrows) relative to the adjacent pancreatic parenchyma. Coronal T1 weighted post-contrast image (**C**) again shows the edge of the hypoenhancing mass (thin arrow) as well as diffuse dilatation of the pancreatic duct throughout the body and tail (block arrows).

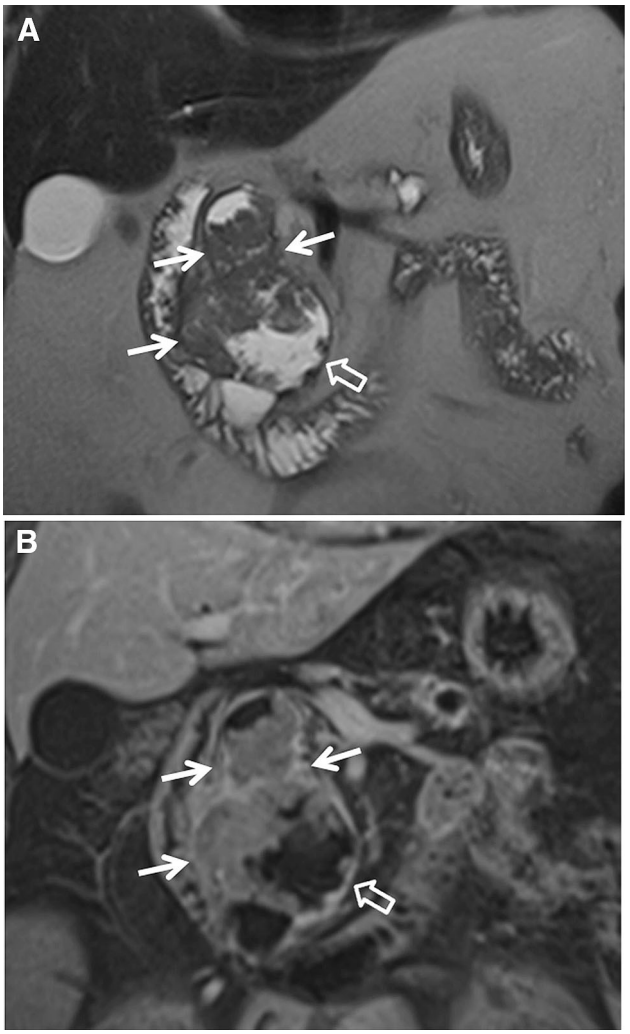

Fig. 2. Coronal T2 weighted image (**A**) and T1 post-contrast image (**B**) demonstrating a large, heterogeneous mass in the pancreatic head (thin arrows) growing within a T2 hyperintense cyst (hollow arrow), consistent with malignant transformation within an intraductal papillary mucinous neoplasm.

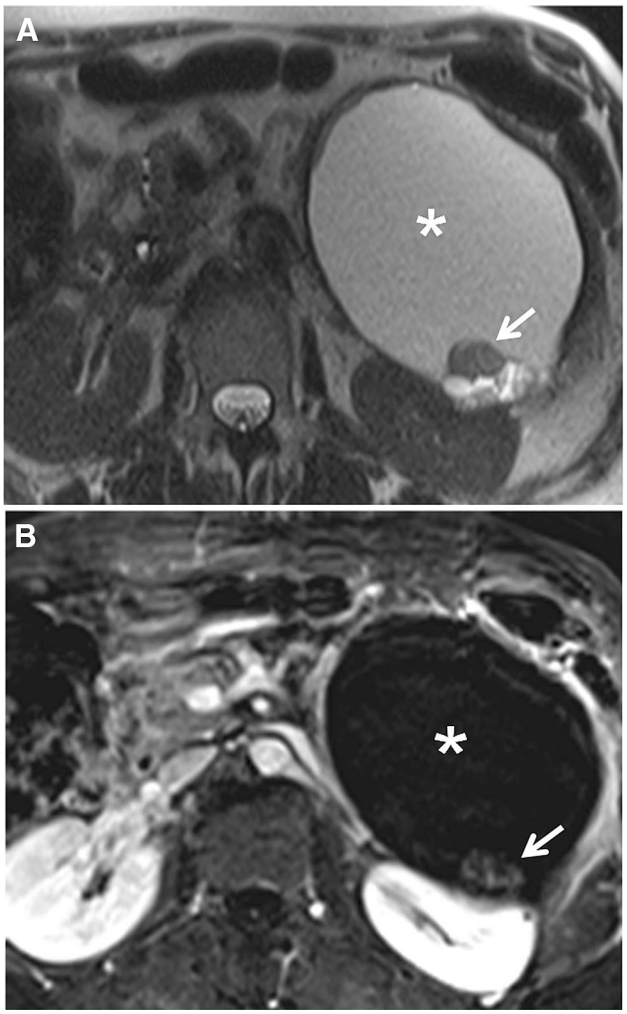

Fig. 3. Axial T2 weighted image (**A**) and motion-corrected subtraction post-contrast image (**B**) demonstrating a large cystic lesion (*) in the pancreatic tail containing a heterogeneous nodule with measurable enhancement (arrow), consistent with adenocarcinoma arising within a mucinous cystic neoplasm, confirmed upon distal pancreatectomy.

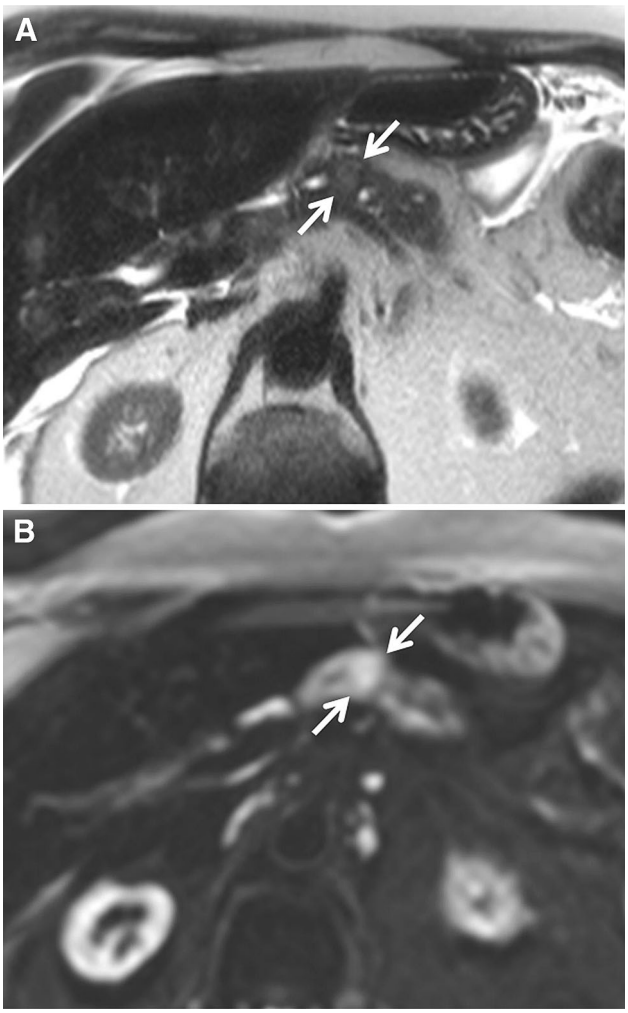

Fig. 4. Axial T2 weighted image (**A**) demonstrating a small area of subtly increased T2 signal (arrows) without significant associated ductal dilatation. Axial high *b*-value diffusion weighted image (**B**) shows a corresponding area of increased diffusion signal (arrows). Decreased signal on the associated attenuation diffusion coefficient (ADC) map confirmed true diffusion restriction (not shown). Subsequent endoscopic ultrasound (EUS) and distal pancreatectomy yielded ductal adenocarcinoma.

However, EUS and biopsy may be necessary to confirm the diagnosis.

Inflammatory pseudotumors, also known as pseudotumoral pancreatitis or mass-forming pancreatitis [10], can arise in the setting of chronic pancreatitis and can be another common cancer mimic. A prior study has estimated that inflammatory pseudotumors may be present in almost 50% of cases of chronic pancreatitis [21]. Differentiating between adenocarcinoma and an inflammatory pseudotumor can be impossible without biopsy, and it can account for 5%–10% of ultimately benign pancreatic resections for presumed malignancy [22]. Like adenocarcinoma, pseudotumors typically appear as a poorly enhancing mass. Unlike cancer, they generally do not cause abrupt duct disruption, instead demonstrating a gradually tapering pancreatic duct as it courses through the mass (the ''duct penetrating sign'') [23].

Lastly, an intrapancreatic splenule can mimic a neoplasm, though more often a neuroendocrine tumor than adenocarcinoma. Intrapancreatic splenules usually can be correctly diagnosed when they demonstrate typical morphology and location in the pancreatic tail. Addi-

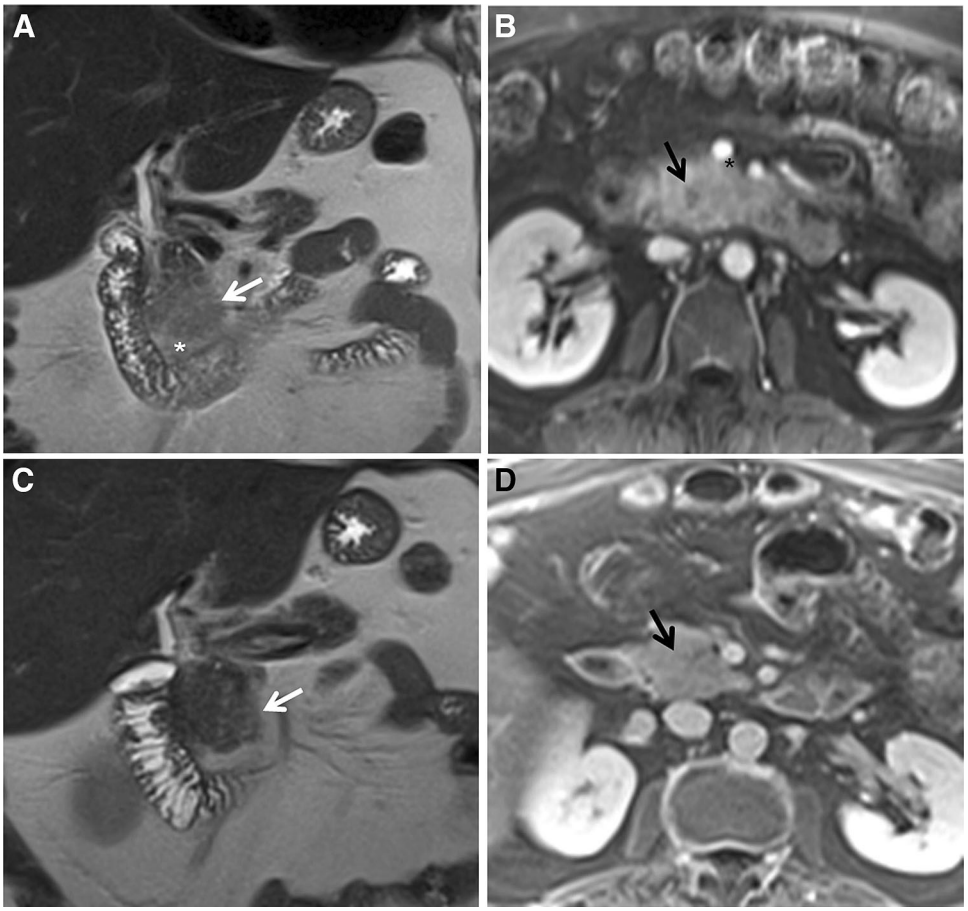

Fig. 5. Coronal T2 weighted image (**A**) demonstrating heterogeneously increased T2 signal within the uncinate process of the pancreas (white arrow) as well as hazy, ill-defined increased signal within the peripancreatic fat inferior to the uncinate (white *). Axial T1 weighted post-contrast image (**B**) demonstrates a small focal area of decreased enhancement in the uncinate (black arrow) as well as abnormal enhancement along the posterior border of the SMV (black *). Follow-up coronal T2 weighted image (**C**) and axial T1 weighted post-contrast image (**D**) 2 months later demonstrate resolution of these findings, consistent with resolved focal pancreatitis in the uncinate.

tionally, MR can be helpful as splenules demonstrate the same signal intensity as the spleen on all sequences [9]. If still uncertain, Tc99m sulfur colloid scan or Tc99m-labeled denatured red blood cell scan can confirm the diagnosis.

Neoplastic mimics

While adenocarcinoma is the most common pancreatic neoplasm, others may demonstrate a similar appearance, especially when small. In these cases, histologic sampling by either EUS and biopsy or surgical resection is required for final tumor diagnosis [15].

Pancreatic neuroendocrine tumors (PNETs) are the second most common primary pancreatic malignancy [24]. They typically occur sporadically but may be seen in genetic syndromes such as multiple endocrine neoplasia type 1, neurofibromatosis type 1, Von Hippel-Lindau, and Tuberous Sclerosis. Similar to adenocarcinoma, PNETs are solid tumors that can cause ductal dilatation and demonstrate diffusion restriction [25]. While PNETs classically demonstrate brisk arterial enhancement, almost 50% of PNETs may not, and these certainly can appear similar to adenocarcinoma (Fig. 7A) [26].Unlike adenocarcinoma, however, PNETs frequently are encapsulated and, accounting for their size and location, may cause less ductal obstruction than adenocarcinoma [27]. Additionally, those PNETs that demonstrate the classic brisk arterial hyperenhancement are easier to accurately diagnose.

Solid-pseudopapillary tumors are uncommon pancreatic neoplasms that are indolent but have malignant

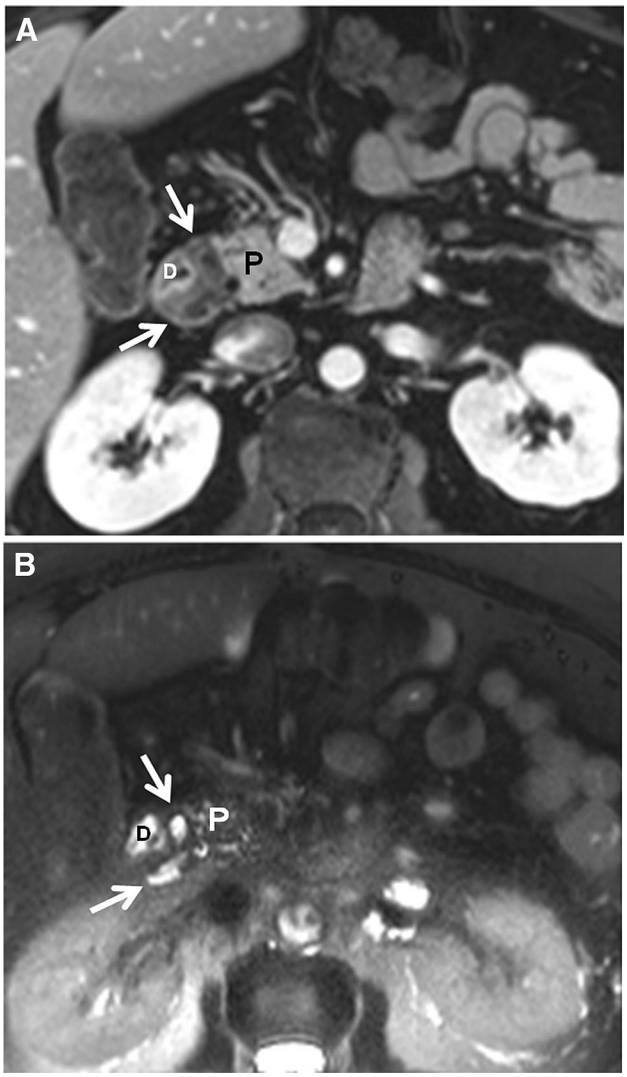

Fig. 6. Axial T1 weighted post-contrast image (**A**) demonstrating a hypoenhancing band (arrows) between the pancreatic head (P) and the second portion of the duodenum (D). Corresponding axial T2 weighed fat-suppressed image (**B**) shows T2 hyperintense cystic structures in the hypoenhancing band (arrows). Findings are consistent with groove pancreatitis, confirmed at surgery.

potential. They generally arise in a specific demographic (women in the second-fourth decade) [28] and most frequently are quite large at presentation, averaging 9 cm in size [29]. Smaller tumors (i.e., less than 3 cm), while less common than their larger counterparts, tend to be solid, homogeneously hypoenhancing masses without a defined capsule, thereby mimicking adenocarcinoma (Fig. 7B) [30]. The lack of significant ductal dilatation and associated parenchymal atrophy may be the only features suggesting against adenocarcinoma. Ultimately, tissue sampling may be required for definitive diagnosis. The more common larger tumors, however, often exhibit both solid and cystic components, hemorrhagic elements, and a defined capsule, thereby posing little diagnostic challenge, particularly in the appropriate patient demographic [15].

Pancreatic acinar cell carcinomas (PACC) are extremely rare exocrine tumors. Affected patients have been known to present with a marked elevation of circulating lipase and may present with polyarthropathy, subcutaneous nodules, and fat necrosis [31]. PACC tumors are also usually large at diagnosis [32, 33], and they often present with metastatic disease [31]. Like solid-pseudopapillary tumors, they are more likely to mimic adenocarcinoma when small, appearing as a solid mass that is hypoenhancing relative to the normal pancreatic parenchyma (Fig. 7C) [32]. They differ from adenocarcinoma by typically being encapsulated, and they usually do not obstruct nearby ducts. The clinical and laboratory presentation can also help lead to the correct diagnosis [31, 32].

Primary pancreatic lymphoma is also rare, generally a B cell type lymphoma., defined as lymphoma in the pancreas and peripancreatic lymph nodes without involvement of superficial lymph nodes, thoracic nodes, or other abdominal organs, and with a normal leukocyte count [33, 34]. While it may exhibit any imaging feature, its most typical appearances are diffuse involvement infiltrating throughout the pancreas and a fairly homogeneous, diffusion restricting mass without ductal dilatation or vascular obstruction [35]. The diffuse form mimics pancreatitis while the focal form mimics adenocarcinoma. Lack of significant ductal obstruction in the setting of a large homogenous mass can aid the radiologist in differentiating between the two.

Metastatic disease to the pancreas accounts for 2%–5% of pancreatic tumors [36]. Tumors that metastasize to the pancreas include renal cell carcinoma most commonly, followed by bronchial carcinoma, melanoma, breast cancer, and colon cancer [9, 15]. The imaging appearance of the metastasis depends on the primary tumor. As with the other pancreas masses described, metastases to the pancreas, when solitary and hypovascular, can mimic pancreatic adenocarcinoma [37]. However, as metastases tend to be multiple in number at the time of diagnosis [9], correctly diagnosing metastatic disease is rarely challenging.

Ampullary adenocarcinomas and periampullary duodenal adenocarcinomas can also masquerade as pancreatic adenocarcinoma. Both are rare tumors arising from the ampulla of vater or duodenal mucosa, respectively [38]. Given their origin, ampullary tumors tend to obstruct nearby ducts, and periampullary duodenal adenocarcinomas may cause ductal obstruction if they are close enough to the ducts. As adenocarcinomas, they

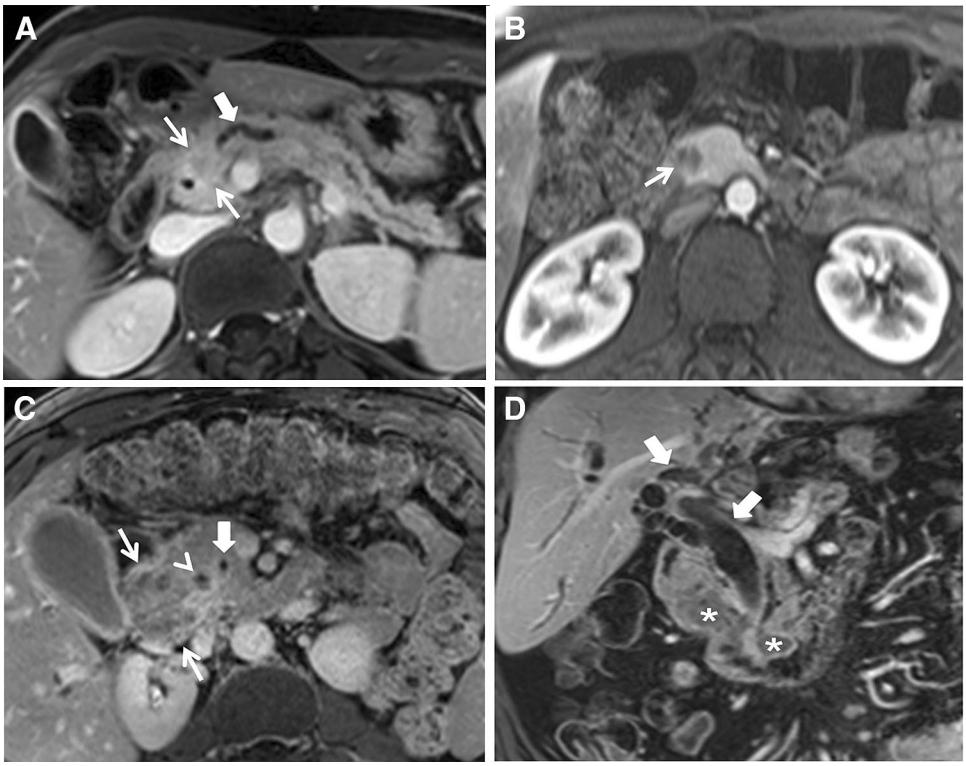

Fig. 7. Neoplastic mimics of pancreas adenocarcinoma. Axial T1 weighted post-contrast image (**A**) showing a hypoenhancing mass (thin arrows) with faint peripheral hyperenhancement. The mass also causes pancreatic duct dilatation (block arrow). EUS-guided biopsy yielded a pancreatic neuroendocrine tumor. Axial T1 weighted post-contrast image (**B**) demonstrates a hypoenhancing mass (arrow) in the pancreatic head. Subsequent pancreaticoduodenectomy confirmed the mass to be a solid-pseudopapillary neoplasm. Axial T1 weighted delayed phase post-contrast image (**C**) illustrates a heterogeneous, infiltrating mass in the pancreatic head (thin arrows) with peripheral enhancement. The mass encroaches upon a stented common bile duct (arrowhead) without significant dilatation of the pancreatic duct (block arrow). EUS-guided biopsy demonstrated pancreatic acinar cell carcinoma. Coronal T1 weighted post-contrast image (**D**) demonstrate a large mass (*) encircling the duodenum at the level of the ampulla causing marked dilatation of both extrahepatic and intrahepatic bile ducts (block arrows). On pathology this tumor was discovered to be an ampullary carcinoma.

Table 2. Summary of AJCC 8th edition TNM staging

T1	Tumor ≤ 2 cm
T1a	Tumor ≤ 0.5 cm
T1b	Tumor > 0.5 cm and < 1 cm
T1c	Tumor 1–2 cm
T2	Tumor > 2 cm and ≤ 4 cm
T3	Tumor > 4 cm
T4	Tumor involves CA, SMA, and/or CHA
N0	No regional lymph node metastases
N1	Regional metastases in 1–3 nodes
N2	Regional metastases in 4 or more nodes
M0	No distant metastases
M1	Distant metastases

AJCC American Joint Committee on Cancer, *TNM* tumor, node, metastasis, *CA* celiac axis, *SMA* superior mesenteric artery, *CHA* common hepatic artery

exhibit signal characteristics and enhancement properties similar to pancreatic adenocarcinoma (Fig. 7D) [39, 40]. As these tumors tend to have a more favorable prognosis than pancreatic adenocarcinoma, distinguishing between the two is significant and often requires histologic sampling [40].

Staging/restaging

Once the diagnosis of pancreatic adenocarcinoma is confirmed, staging of the disease and evaluation for surgical resectability become paramount. The tumor, node, metastases (TNM) system from the American Joint Committee on Cancer (AJCC) is the preferred system for staging (Table 2) [41]. Its recent 8th edition classifies the T stage based on the size of the tumor and whether or not critical peripancreatic vascular structures, such as the superior mesenteric artery (SMA), celiac axis, or common hepatic artery, are involved. Nodal disease is stratified not only on the presence of involved regional lymph node metastases, but also on the actual number of nodes involved. Most critical remains the presence or

Table 3. NCCN 2017 resectability criteria based on peripancreatic vascular involvement

Resectability	Arterial involvement	Venous involvement
Resectable	No contact (CA, SMA, CHA)	No contact or < 180 (SMV, PV)
Borderline resectable	-GDA encasement up to the hepatic artery with either short segment encasement or direct abutment of the hepatic artery without extension to the CA -Tumor abutment of the SMA or CA (< 180)	Involvement of the SMV or portal vein (distortion, narrowing, or occlusion) with suitable vessel proximal and distal, allowing for safe resection and replacement
Unresectable	-Aortic or IVC invasion or encasement -≥ 180° SMA encasement -Involvement of first jejunal SMA branch	-Unreconstructable SMV/portal vein -Involvement of draining jejunal branch into SMV

NCCN National Comprehensive Cancer Network, *CA* celiac axis, *SMA* superior mesenteric artery, *CHA* common hepatic artery, *GDA* gastroduodenal artery, *SMV* superior mesenteric vein, *PV* portal vein, *IVC* inferior vena cava

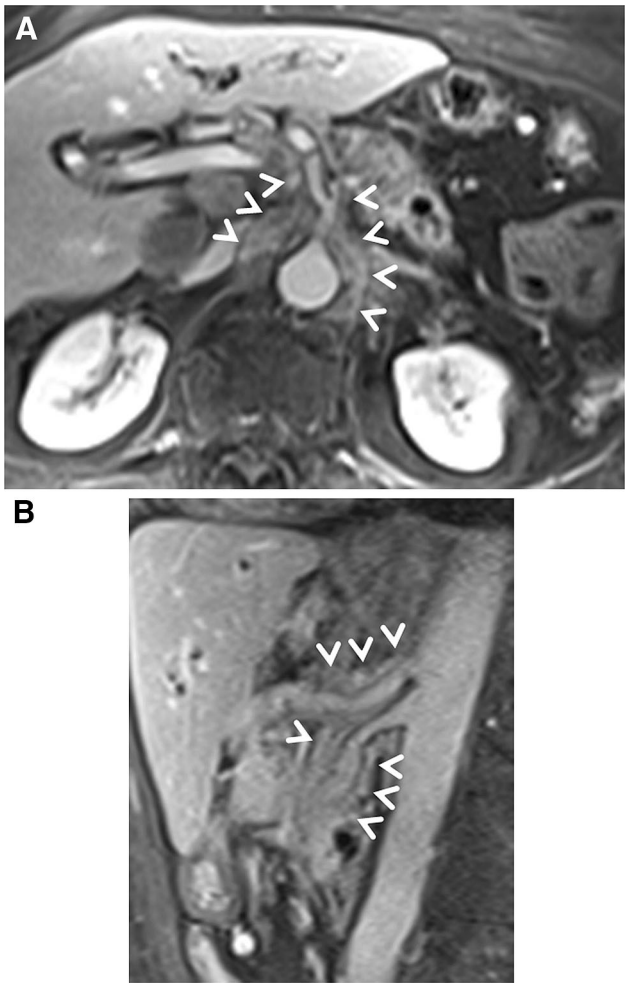

Fig. 8. Axial (**A**) and sagittal (**B**) T1 weighted post-contrast images showing unresectable disease, with abnormal soft tissue (arrowheads) encasing both the celiac axis and SMA, as well as near-encasement of the abdominal aorta. Note how the single sagittal image (**B**) clearly outlines tumor involvement along the proximal celiac artery and SMA.

Fig. 9. Axial T1 weighted post-contrast image demonstrating a hypoenhancing mass (*) in the pancreatic head with abnormal soft tissue abutting the posterior margin of the SMV (small white arrow) and SMA (small black arrow). There is less than 180° involvement of both vessels. In the absence of known metastatic disease, these findings render the tumor borderline resectable, and the patient underwent chemoradiation. Also noted is a common bile duct stent (S).

absence of distant metastatic disease, as the presence of any metastases precludes surgical treatment.

In terms of potential surgical management of disease, the National Comprehensive Cancer Network typically divides pancreatic adenocarcinoma into three categories: resectable, borderline resectable, and unresectable (Table 3) [42–44]. In general, tumor resectability relies upon its relationship with adjacent vessels, particularly the SMA, celiac axis, hepatic artery, portal vein, superior mesenteric vein (SMV), aorta, inferior vena cava (IVC), and first jejunal artery and vein. The greater the involvement of the peripancreatic vasculature, the less likely the tumor can be resected with negative margins. Tumors with no vessel involvement or distant metastases are generally resectable (Fig. 1). Tumors with encasement of critical vessels, such as the SMA and its primary branches, are unresectable, with encasement described as involving more than 180° of the vessel circumference (Fig. 8). Borderline resectable tumors generally abut vessels, described as involving less than 180° of the vessel circumference (Fig. 9). However, tumors

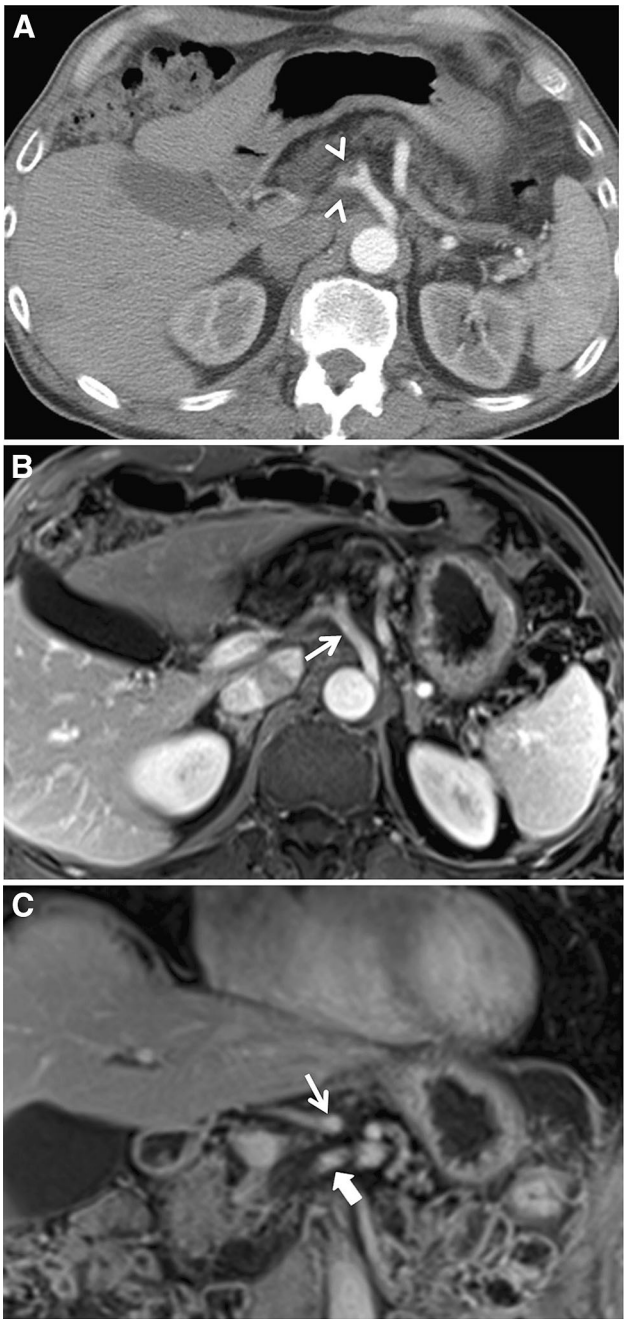

Fig. 10. Axial contrast-enhanced CT image (**A**) in a patient with a known pancreatic head tumor (not shown) demonstrating ill-defined density around the celiac bifurcation (arrowheads), suspicious for tumor involvement. Axial (**B**) and coronal (**C**) T1 weighted post-contrast images of a subsequent MR exam 4 weeks later with no interval treatment demonstrate no tumor involvement about the celiac axis (thin arrow) or SMA (block arrow). This patient proceeded to pancreaticoduodenectomy with negative surgical margins.

with short-segment encasement of the portal vein, SMV, or even the celiac axis or hepatic artery may be borderline resectable as well. The resectability of such tumors

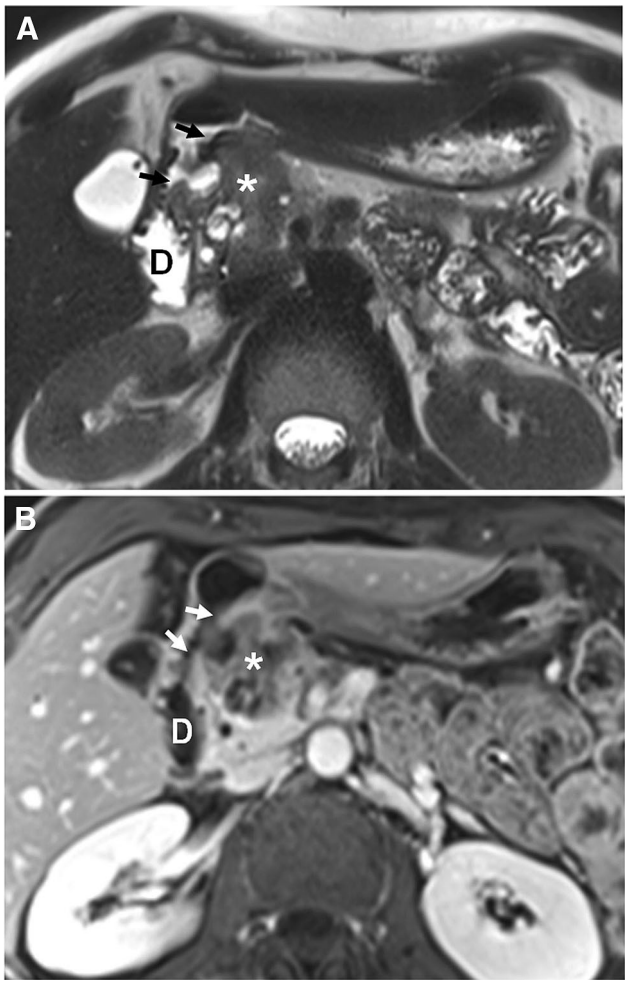

Fig. 11. Axial T2 weighed image (**A**) and T1 weighted post-contrast image (**B**) demonstrating a large hypoenhancing mass in the pancreatic head (*) with direct invasion of the wall (small arrows) of the duodenum (D).

frequently depends on the length of encasement, suitability for vascular reconstruction, and skill of the surgeon. Detailed discussion with the referring surgeon is always recommended as newer surgical approaches continue to evolve [45, 46].

While studies have shown comparable accuracy between CT and MR in correctly staging the degree of vascular involvement [5], the limited soft-tissue contrast inherent in CT sometimes leads to overestimation of perivascular tumor spread (Fig. 10). As previously discussed, the multiple MR sequence types also afford the radiologist several opportunities to prove or disprove vascular involvement. In particular, sequences acquired in the coronal and sagittal planes can be invaluable in correctly identifying or confirming the extent of vascular involvement (see Figs. 8B and 10C). Equally important is detection of any vascular anatomic variants, most commonly involving the hepatic artery or its branches arising from the SMA or left gastric artery, to minimize the

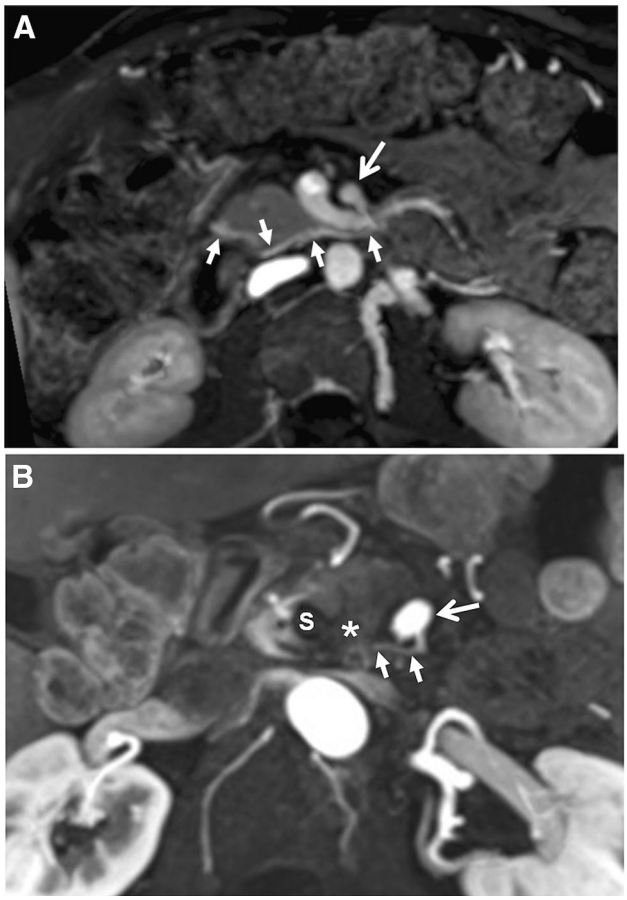

Fig. 12. Oblique axial thin arterial phase T1 weighted post-contrast maximum intensity projection (MIP) images of the posterior inferior pancreaticoduodenal artery (PIPDA, small arrows) arising from the SMA (larger arrow), around normal uncinate parenchyma (**A**) and a hypointense adenocarcinoma (*) in the pancreatic head (**B**). The cancer involves the PIPDA, an imaging biomarker for extrapancreatic perineural invasion. Common bile duct stent (S) is also present in (**B**).

chance of injury during surgery or to identify unexpected tumor involvement of an anatomic variant. Coronal and sagittal images are useful in this regard as well. More recent literature has also highlighted imaging biomarkers for aggressive tumor biology, such as duodenal invasion and extrapancreatic perineural invasion [47–49]. Similar to CT, MR can accurately identify the presence of both (Figs. 11 and 12).

Additionally, the evaluation for advanced locoregional disease also includes assessment for abnormal regional lymph nodes and for invasion of other adjacent organs. With the exception of the spleen, tumor invasion of any adjacent organ affects surgical resectability [43, 45]. Regional lymph node involvement confirms advanced locoregional disease, while more remote nonregional lymph node involvement, such as in inferior retroperitoneal nodes, infrarenal nodes, or jejunal

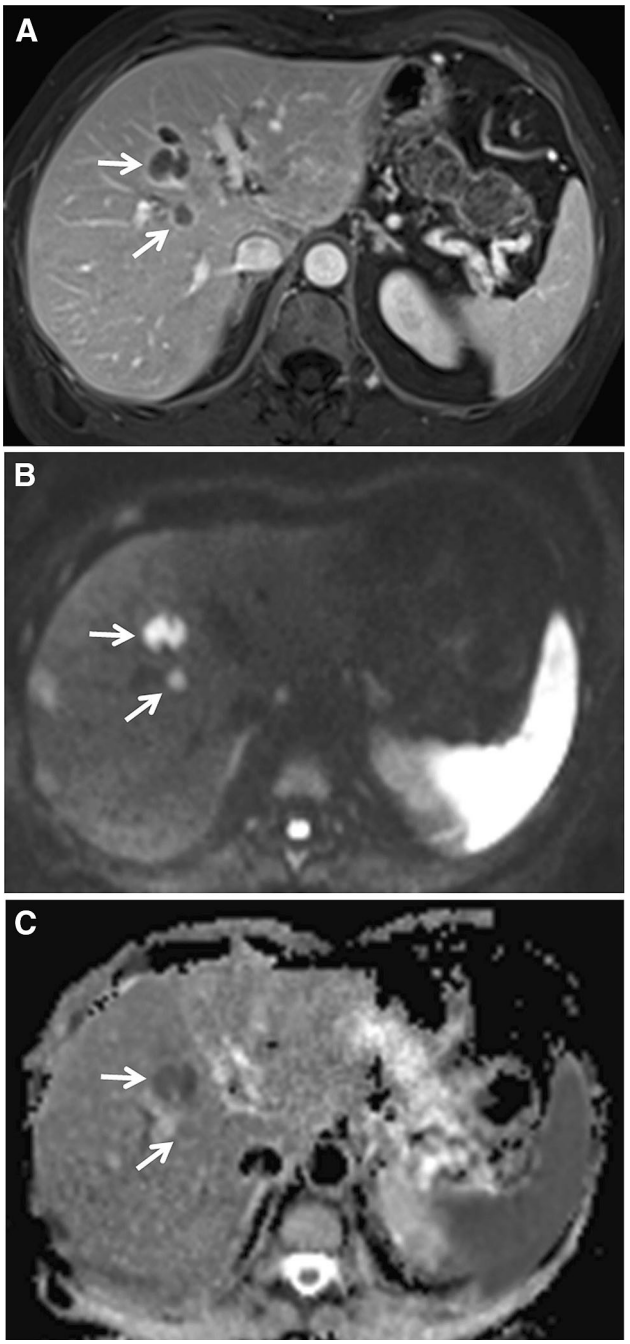

Fig. 13. Axial T1 weighted post-contrast image (**A**), high *b*-value diffusion weighted image (**B**), and ADC map image (**C**) in a patient with known pancreatic adenocarcinoma demonstrate multiple hypointense, peripherally enhancing lesions with associated restricted diffusion in the right hepatic lobe, consistent with metastatic disease.

mesenteric lymph nodes, equates to distant metastatic disease.

The most common site for pancreatic metastases is the liver. Previous studies have demonstrated that MRI is superior to CT in the detection of liver metastases due to a combination of multiphase contrast sequences plus

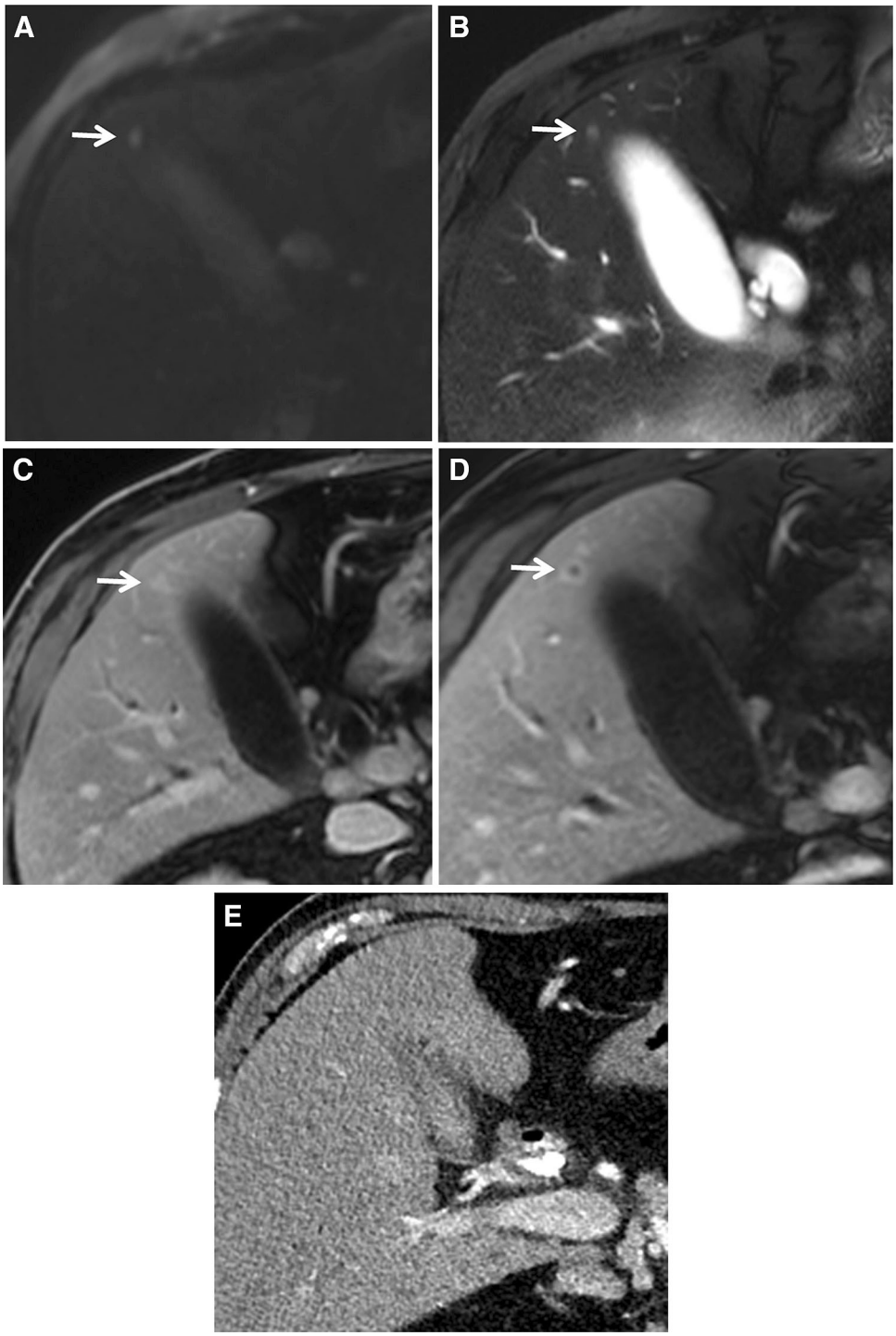

Fig. 14. An example highlighting the power of the thin arterial phase T1 weighted sequences with higher flip angle in evaluating small liver lesions in a patient with known pancreatic adenocarcinoma. Axial high *b*-value diffusion weighted image (**A**) and axial T2 weighted fat-suppressed image (**B**) demonstrate a small focus of increased diffusion and T2 signal near the gallbladder fossa (arrows). This focus was too small to appreciate on ADC map (not shown). Axial T1 post-contrast image from the portal venous phase (**C**) demonstrates fairly homogeneous, low-level enhancement. Based on these findings, it is impossible to determine whether this represents a metastasis or a small benign hemangioma. However, the thin axial arterial phase T1 weighted post-contrast image (**D**) clearly demonstrates suspicious ring-enhancement, most suggestive of a metastasis. This was subsequently confirmed on follow-up MR exams which demonstrated progression of metastatic disease despite treatment (not shown). Axial contrast-enhanced CT image (**E**) performed one month after the initial MR exam shows no detectable liver lesion despite its confirmed presence on the earlier MR and subsequent MR exams (not shown).

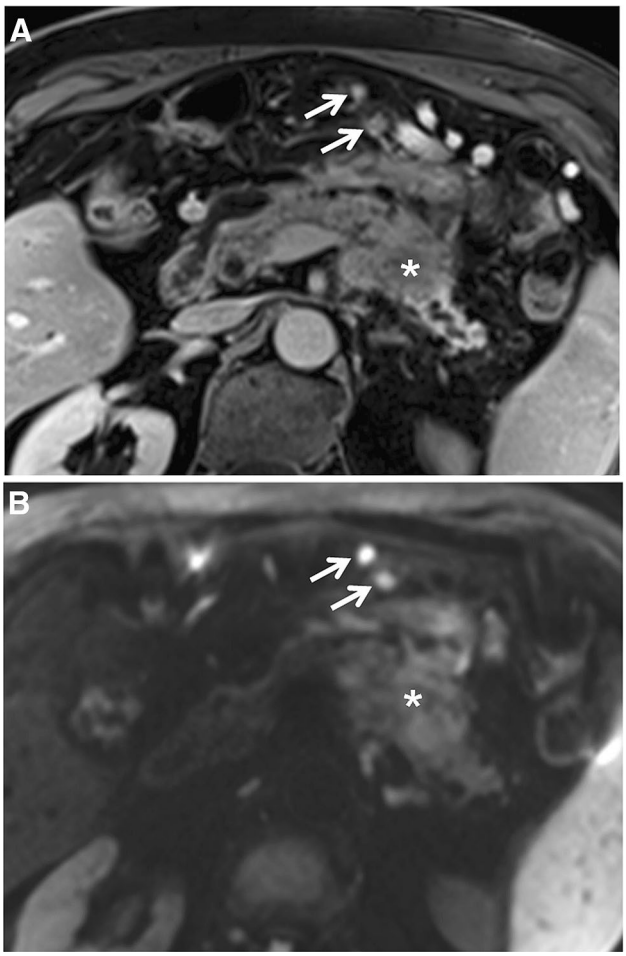

Fig. 15. Axial T1 post-contrast image (**A**) showing an expansile mass (*) in the pancreatic body/tail causing pancreatic duct dilatation in the tail. There are two visible soft-tissue implants in the omentum (arrows), consistent with carcinomatosis. The omental implants are much more conspicuous on the corresponding axial high *b*-value diffusion weighted image (**B**). Note that it is not unusual for tumor implants and metastases to have higher signal on diffusion weighted images than the primary tumor, as in this case.

diffusion weighted imaging (DWI) (Fig. 13) [8, 50]. Small metastases are much more readily identified on MR. Moreover, because of the disparate imaging characteristics targeted by the various sequences, an occult or indeterminant CT lesion often can be definitively diagnosed [51]. In particular, we have found that the thin arterial phase T1 weighted sequences with higher flip angle that we run through the liver often allow for improved detection and characterization of these small metastases, even compared to other post-contrast sequences (Fig. 14).

After the liver, the most common site for metastatic disease is the peritoneum [42]. MR is known to be highly effective in the detection of peritoneal disease, though most published studies highlight this utility in ovarian cancer [52, 53]. Similar to others [6, 53], we have found that MR is adept at diagnosing peritoneal metastases from pancreas adenocarcinoma. Peritoneal implants typically demonstrate intermediate T1 and T2 signal intensity and can be obscured if adjacent to other abdominal organs or bowel. However, they are frequently more conspicuous on post-contrast and DWI sequences, especially when small (Fig. 15).

Patients with unresectable or borderline resectable disease at diagnosis undergo neoadjuvant chemotherapy and/or radiation with subsequent imaging surveillance to monitor response to treatment. Interpretation of these follow-up exams often is challenging [54]. While many tumors demonstrate some response to treatment, either as diminished size or decreased diffusion restriction, complete resolution of abnormal signal or enhancement about involved peripancreatic vessels is rare. In one recent trial, only 4% of patients initially diagnosed with unresectable disease responded to neoadjuvant therapies well enough to proceed to surgical resection [55]. However, complete or near-complete responses do occur, typically in borderline resectable cases (Fig. 16). More commonly, distinguishing residual viable perivascular tumor from perivascular fibrosis can be problematic. Often, a clinical decision will be based on additional considerations, such as the response of the original tumor, tumor serum markers (such as carbohydrate antigen 19-9), and the overall condition of the patient [56]. In our institution, if there is dramatic response to therapy of the primary tumor and near resolution of the abnormal soft tissue surrounding nearby vessels, the surgeon may opt for EUS or exploratory surgery to confirm or exclude residual perivascular tumor involvement. If no tumor is confirmed, the case will proceed to definitive resection. In our practice, this stepwise treatment scheme has led to several resections with negative margins, despite persistent perivascular soft tissue on immediate pre-operative MR exams.

Conclusion

Despite recent advances in imaging technology, accurate diagnosis and staging of pancreas adenocarcinoma remains difficult. In our institution, MRI has become the standard imaging modality for the diagnosis and staging of pancreatic adenocarcinoma. As more recent studies highlight the importance of specific imaging biomarkers in the prognosis of the disease, MR has proven well suited to detect them. As newer treatment regimens for

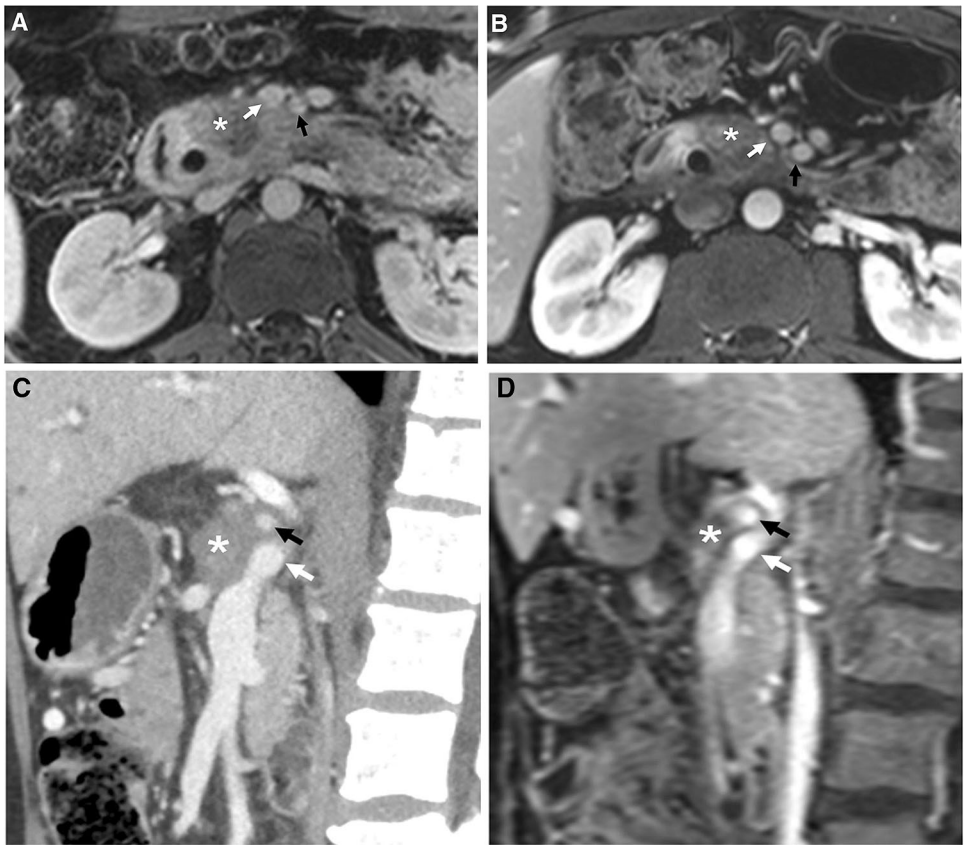

Fig. 16. Two examples of tumor response to neoadjuvant therapy. Axial T1 post-contrast images before (**A**) and after (**B**) chemoradiation treatment. The image in (**A**) is the same as in Fig. 9. Post-treatment image (**B**) demonstrates decrease in size of the primary pancreatic tumor (*) and complete tumor regression from the SMV and SMA (small white and black arrow, respectively), as well as regression from the duodenum. This patient subsequently proceeded to pancreaticoduodenectomy with negative surgical margins and no vascular involvement. Sagittal contrast-enhanced CT image (**C**) of another patient demonstrates tumor encasement (*) of the hepatic artery (small black arrow) and the portal confluence (small white arrow). Post-treatment sagittal T1 post-contrast MR image (**D**) demonstrates substantial decrease in abnormal soft tissue about the hepatic artery and portal confluence. Given the patient's morphologic and biochemical response, she proceeded to total pancreatectomy, with negative surgical margins and no viable tumor identified along the peripancreatic vasculature.

locally advanced and metastatic disease continue to emerge, we expect MR imaging to become increasingly essential in accurately assessing disease burden, therapeutic options, and treatment response.

Acknowledgements The authors would like to acknowledge Dr. Mellena Bridges for inspiration and Dr. David DiSantis for assistance in manuscript preparation.

Compliance with ethical standards

Conflict of interest The authors declare that they have no conflict of interest.

References

1. American Cancer Society. https://cancerstatisticscenter.cancer.org/?_ga=2.223842450.801427553.1527536019-1868478499.1527536019#!/cancer-site/Pancreas. Accessed 28 May 2018
2. National Cancer Institute. SEER cancer statistics factsheets: pancreas cancer. http://seer.cancer.gov/statfacts/html/pancreas.html. Accessed 21 Feb 2018
3. Croome KP, Jayaraman S, Schlachta CM (2010) Preoperative staging of cancer of the pancreatic head: is there room for improvement? Can J Surg 53:171–174
4. Kambadakone AR, Zaheer A, Le O, et al. (2018) Multi-institutional survey on imaging practice patterns in pancreatic ductal adenocarcinoma. Abdom Radiol 43:245–252
5. Chen F, Ni J, Zhang Z, et al. (2016) Presurgical evaluation of pancreatic cancer: a comprehensive imaging comparison of CT vs. MRI. AJR Am J Roentgenol 206:526–535
6. Miller FH, Rini NJ, Keppke AL (2006) MRI of adenocarcinoma of the pancreas. Am J Roentgenol 187(4):W365–W374
7. Kulkarni NM, Hough DM, Tolat PP, et al. (2018) Pancreatic adenocarcinoma: cross-sectional imaging techniques. Abdom Radiol 43:253–263
8. Motosugi U, Ichikawa T, Morisaka H, et al. (2011) Detection of pancreatic carcinoma and liver metastases with gadoxetic acid-enhanced MR imaging: comparison with contrast-enhanced multidetector row CT. Radiology 260(2):446–453
9. Bridges MD (2015) Magnetic resonance imaging of pancreatic malignancy. Transl Cancer Res 4(6):616–633
10. Low G, Panu A, Millo N, et al. (2011) Multimodality imaging of neoplastic and non-neoplastic solid lesions of the pancreas. Radiographics 31:993–1015
11. Tanaka M, Fernández-del Castillo C, Adsay V, et al. (2012) International consensus guidelines 2012 for the management of IPMN and MCN of the pancreas. Pancreatology 12:183–197

12. Manfredi R, Ventriglia A, Mantovani W, et al. (2015) Mucinous cystic neoplasms and serous cystadenomas arising in the body-tail of the pancreas: MR imaging characterization. Eur Radiol 25:940–949
13. Kim SH, Lee JM, Lee ES, et al. (2015) Intraductal papillary mucinous neoplasms of the pancreas: evaluation of malignant potential and surgical resectability by using MR imaging with MR cholangiography. Radiology 274:723–733
14. Le Baleur Y, Couvelard A, Vuillierme MP, et al. (2011) Mucinous cystic neoplasms of the pancreas: definition of preoperative imaging criteria for high-risk lesions. Pancreatology 11:495–499
15. Gandhi NS, Feldman MK, Le O, et al. (2018) Imaging mimics of pancreatic ductal adenocarcinoma. Abdom Radiol 43:273–284
16. Siddiqi AJ, Miller F (2007) Chronic pancreatitis: ultrasound, computed tomography, and magnetic resonance imaging features. Semin Ultrasound CT MR 28(5):384–394
17. Raman SP, Horton KM, Cameron JL, et al. (2013) Groove pancreatitis: spectrum of imaging findings and radiology-pathology correlation. Am J Roentgenol 201(1):2–13
18. Blasbalg R, Baroni RH, Costa DN, et al. (2007) MRI features of groove pancreatitis. Am J Roentgenol 189:73–80
19. Okazaki K, Uchida K, Koyabu M, et al. (2011) Recent advances in the concept and diagnosis of autoimmune pancreatitis and IgG4-related disease. J Gastroenterol 46(3):277–288
20. Sahani DV, Kalva SP, Farrell J, et al. (2004) Autoimmune pancreatitis: imaging features. Radiology 233:345–352
21. Kroft SH, Stryker SJ, Winter JN, et al. (1995) Inflammatory pseudotumor of the pancreas. Int J Pancreatol 18:277–283
22. Tajima Y, Kuroki T, Tsutsumi R, et al. (2007) Pancreatic carcinoma coexisting with chronic pancreatitis vs. tumor-forming pancreatitis: diagnostic utility of the time-signal intensity curve from dynamic contrast-enhanced MR imaging. World J Gastroenterol 13(6):858–865
23. Ichikawa T, Sou H, Araki T, et al. (2001) Duct-penetratign sign at MRCP: usefulness for differentiating inflammatory pancreatic mass from pancreatic carcinomas. Radiology 221:107–116
24. National comprehensive cancer network clinical practice guidelines in oncology: neuroendocrine tumors version 3.2017. Accessed 13 June 2017
25. Wang Y, Chen ZE, Yaghmai V, et al. (2011) Diffusion-weighted MR imaging in pancreatic endocrine tumors correlated with histopathologic characteristics. J Mag Reson Imaging 33:1071–1079
26. Jeon SK, Lee JM, Joo I, et al. (2017) Nonhypervascular pancreatic neuroendocrine tumors: differential diagnosis from pancreatic ductal adenocarcinomas at MR imaging—retrospective cross-sectional study. Radiology 284(1):77–87
27. Kim JH, Eun HW, Kim YJ, et al. (2016) Pancreatic neuroendocrine tumor (PNET): staging accuracy of MDCT and its diagnostic performance on PNET with uncommon CT findings from pancreatic adenocarcinoma. Eur Radiol 26:1338–1347
28. Marchegiani G, Andrianello S, Massignani M, et al. (2016) Solid pseudopapillary tumors of the pancreas: specific pathological features predict the likelihood of postoperative recurrence. J Surg Oncol 114(5):597–601
29. Beutow PC, Buck JL, Pantongrag-Brown L, et al. (1996) Solid and papillary epithelial neoplasm of the pancreas: imaging-pathologic correlation on 56 cases. Radiology 199(3):707–711
30. Ganashan DM, Paulson E, Tamm EP, et al. (2013) Solid pseudopapillary tumors of the pancreas: current update. Abdom Imaging 38:1373–1382
31. Barral M, Faraoun SA, Fishman EK, et al. (2016) Imaging features of rare pancreatic tumors. Diagnos Interv Imaging 97:1259–1273
32. Tatli S, Mortele KJ, Levy AD, et al. (2005) CT and MRI features of pure acinar cell carcinoma of the pancreas. Am J Roentgenol 184:511–519
33. Steinman J, Zaheer A, Kluger MD, et al. (2018) Rare pancreatic tumors. Abdom Radiol 43:285–300
34. Dawson IM, Cornes JS, Morson BC (1961) Primary malignant lymphoid tumors of the intestinal tract. Report of 37 cases with a study of factors influencing prognosis. Br J Surg 49:80–89
35. Merkle EM, Bender GN, Brambs HJ (2000) Imaging findings in pancreatic lymphoma: differential aspects. Am J Roentgenol 174(3):671–675
36. Tsitouridis I, Diamantopoulou A, Michaelides M, et al. (2010) Pancreatic metastases: CT and MRI findings. Diagnos Interv Radiol 16(1):45–51
37. Ahmed S, Johnson PT, Hruban R, et al. (2013) Metastatic disease to the pancreas: pathologic spectrum and CT patterns. Abdom Imaging 38:144–153
38. Nikolaidis P, Hammond NA, Day K, et al. (2014) Imaging features of benign and malignant ampullary and periampullary lesions. Radiographics 34:624–641
39. Kim TU, Kim S, Lee JW, et al. (2008) Ampulla of Vater: comprehensive anatomy, MR imaging of pathologic conditions, and correlation with endoscopy. Eur J Radiol 66(1):48–64
40. Kim JH, Kim MJ, Chun JJ, et al. (2002) Differential diagnosis of periampullary carcinomas at MR imaging. Radiographics 22(6):1335–1352
41. AJCC Cancer Staging Manual (2016) 8th edn. Springer, ISBN 978-3-319-40617-6.
42. Soloff EV, Zaheer A, Meier J, et al. (2018) Staging of pancreatic cancer: resectable, borderline resectable, and unresectable disease. Abdom Radiol 43:301–313
43. https://www.nccn.org/professionals/physician_gls/pdf/pancreatic.pdf.
44. Al-Hawary MM, Francis IR, Chari ST, et al. (2014) Pancreatic ductal adenocarcinoma radiology reporting template: consensus statement of the Society of Abdominal Radiology and the American Pancreatic Association. Radiology 270(1):248–260
45. Fonseca AL, Fleming JB (2018) Surgery for pancreatic cancer: critical radiologic findings for clinical decision making. Abdom Radiol 43:374–382
46. Javid AA, Bleich K, Bagante F, et al. (2017) Pancreaticoduodenectomy with venous resection and reconstruction: current surgical techniques and associated postoperative imaging findings. Abdom Radiol . https://doi.org/10.1007/s00261-017-1290-5
47. Chang ST, Jeffrey RB, Patel BN, et al. (2016) Preoperative multidetector CT diagnosis of extrapancreatic perineural or duodenal invasion is associated with reduced postoperative survival after pancreaticoduodenectomy for pancreatic adenocarcinoma: preliminary experience and implications for patient care. Radiology 281:816–825
48. Patel BN, Olcott E, Jeffrey RB (2018) Extrapancreatic perineural invasion in pancreatic adenocarcinoma. Abdom Radiol 43:323–331
49. Patel BN, Olcott EW, Jeffrey RB (2018) Duodenal invasion by pancreatic adenocarcinoma: MDCT diagnosis of an aggressive imaging phenotype and its clinical implications. Abdom Radiol 43:332–339
50. Holzapfel K, Reiser-Erkan C, Fingerle AA, et al. (2011) Comparison of diffusion-weighted MR imaging and multidetector-row CT in the detection of liver metastases in patients operated for pancreatic cancer. Abdom Imaging 36:179–184
51. Bhalla M, Aldakkak M, Kulkarni NM, et al. (2018) Characterizing indeterminate liver lesion in patients with localized pancreatic cancer at the time of diagnosis. Abdom Radiol 43: 351–363
52. Low RN, Carter WD, Saleh F, et al. (1995) Ovarian cancer: comparison of findings with perfluorocarbon-enhanced MR imaging, In-111-CYT-103 immunotherapy, and CT. Radiology 195(2):391–400
53. Low RN (2007) MR imaging of the peritoneal spread of malignancy. Abdom Imaging 32:267–283
54. Baliyan V, Kordbacheh H, Parakh A, et al. (2018) Response assessment in pancreatic ductal adenocarcinoma: role of imaging. Abdom Radiol 43:435–444
55. Hammel P, Huguet F, van Laethem JL, et al. (2016) Effect of chemoradiotherapy vs chemotherapy on survival in patients with locally advanced pancreatic cancer controlled after 4 months of gemcitabine with or without erlotinib: the LAP07 randomized clinical trial. JAMA 315(17):1844–1853
56. Bergquist JR, Puig CA, Shubert CR, et al. (2016) Carbohydrate antigen 19-9 elevation in anatomically resectable, early stage pancreatic cancer is independently associated with decreased overall survival and an indication for neoadjuvant therapy: a national cancer database study. J Am Coll Surg 223(1):52–65